

EXPERIMENTAL STUDIES ON MILLIMETER WAVE AND INFRARED PROPAGATION IN ARID CLIMATE

Adel A. Ali, Mohammed A. Alhaider and Abobakr S. Ahmed

College of Engineering, King Saud University, Saudi Arabia

INTRODUCTION

A field study on wave propagation covering a wide range of the electromagnetic spectrum has been actively running for the last three years period in Riyadh region, Saudi Arabia. This region can be considered a typical arid climate. This paper reports the first set of data obtained by measuring the received signal variations on millimeter wave and near infrared links during this year. In particular, the effects of airborne dust, rain and turbulence on propagations are presented and discussed.

THE EXPERIMENTAL SYSTEM

A block diagram of the experimental system is shown in Figure 1. The system comprises (I) a set of five transmission links operating at microwave (~12.5 GHz), millimeter wave MMW (~40 GHz) and near infrared NIR (0.880 μm) with different path distances of 14 km, 10 km and 0.75 km. (II) Meteorological instrumentation situated at the receiving site; which includes dust passive collectors (DPC) and high volume samplers (HVS) at different heights above ground, along with particle-size analyser (PSA), for measuring airborne dust parameters. A rainfall rate gauge (RRG) and meteorological station (MS) for the measurement of temperature (T), relative humidity (RH), wind speed and direction (ws, wd) and barometric pressure (P). (III) a data collection and processing laboratory which includes a minicomputer (μc), tape (t_p), printer, data acquisition system (DAS), 40 GHz spectrum analyzer (SA) and multichannel recorders (MCR).

Parameters of the link systems

Parameter	BKM	HU/HUP	NEC	NIR
Transmitter frequency (GHz)	12.465	39.306/39.434	38.925	0.880 μm
Transmitted power (dBm)	+20	+23	+10	+14.77
Transmitter	x-tal	DRO & Impatt	Impatt	Ga Al As
Polarization	Vertical	Vertical	Vertical	Random
Antenna type, and gain (dB)	Parabola, 35	Cassegrain, 35	Cassegrain, 40	Fresnel lens
First IF (GHz)	0.430	1.142/1.27	1.70	-
Second IF (MHz)	70	300	70	-
Bandwidth (MHz)	19	42.5	35	40 nm
AGC range (dB)	45	30	50	30
BB signal used	1 MHz	1/2 MHz	2 MHz	TV Colour
Path distance (km)	14	14/10	14	0.75
Fade margin (dB)	30	15/25	15	10
Elevation angle ($^{\circ}$)	0.029	0.029/0.017	0.029	0.3
Azimuth ($^{\circ}$)	135	135, 120	135	270

The following Table lists the basic parameters of the different links. The paths are partly over open arid area and partly over an urban area of Riyadh city. Path clearances are much larger than the first Fresnel zone at all frequencies and everywhere.

EXPERIMENTAL RESULTS

Airborne Dust-Event

Figure 2 shows an example of a blown dust event occurred on February 2, 1986, between 16:30 and 17:45 local time. The optical visibility $V_0 = 3.75$ km which was measured using the NIR link attenuation i.e. $V_0 \alpha_0 = 1.5$ (Middleton (1)). Other meteorological parameters were: $T = 25^{\circ}\text{C}$, $\text{RH} = 59\%$, $w_s = 18 \text{ m.s}^{-1}$, $w_d = 310^{\circ}$ and water vapour concentration $v = 5.89 \text{ g.m}^{-3}$. The dust-induced fades did not exceed 1 dB on MMW links and 3 dB on the NIR link. However it is noticed that the shape of the fades are different. While on the NIR link, it is similar to rain-induced fade, the shape of the fade on the MMW link exhibits rapid fluctuations of the nominal level.

Dust-Attenuation Statistics

Figure 3 shows the distribution of the attenuation coefficient α (dB.km^{-1}) due to the propagation of MMW and NIR wave through airborne dust. For example for 0.1% of the year the attenuation α may exceed 0.036 dB.km^{-1} and 5.5 dB.km^{-1} at 40 GHz and 0.880 μm respectively. The higher attenuation at 0.880 μm compared with that at 40 GHz may be explained by the higher ratio of the particle

size to wavelength. Consequently the normalised extinction cross section is much higher at 0.880 μm (actually it is equal to 2). The measured results A_m of the MMW links are compared with the calculated values A_c by Ansari and Evans (2), assuming that the 14 km path is completely filled with airborne dust. For the high bound of moisture content $w = 20\%$ and average particle radius $a=50 \mu\text{m}$, it is found that $A_c = 0.76 \text{ dB}$ and 1.43 dB at $V_0 = 3.75 \text{ km}$ and 0.6 km respectively. The corresponding measured values are 1 dB and 2 dB . It is likely that other distributions than the assumed exponential might exist and the assumed values of soil permittivity in reference (2) are not appropriate.

Rain-Event

Figure 4 shows an example of the measured effect of rain event on the 40 GHz, 14 km and the 0.880 μm , 0.75 km links. The experimental data indicates that the correlation between the rainfall rate and the measured fade is quite good. This correlation was evident by checking the linear proportionality between the measured one-minute rainfall rate at the receiving site and the measured average path attenuation on log-log plot.

Rain-Attenuation Statistics

Figure 5 shows the measured attenuation coefficient due to rainfall at 0.880 μm assuming rain cell size $> 0.75 \text{ km}$. At infrared wavelength α_0 can be calculated from the equation (Zeuv (3)): $(\alpha_0) = 0.912 R^{0.74} (\text{dB.km}^{-1})$ where R is the rainfall rate in mm.h^{-1} . The agreement between measurement and calculation using the above equation is within experimental error. The maximum difference is 0.8 dB.km^{-1} approximately.

Figure 6 represents the measured distribution of rainfall attenuation for the MMW link and the measurement is compared with calculation. The calculation is based on the well known aR^b relation (Olsen et al (4)) where $a = 0.313$ and $b = 0.981$ at 40 GHz, rain temperature of 20°C and assuming average rain cell size according to CCIR Rep. 563-1. The agreement between measured and calculated distributions is observed at higher rainfall rate, while the calculated values are higher than the measured values at lower rainfall rate. This may be due to the assumed cell size are obtained for heavy rainfall climate.

Amplitude Scintillations in MMW

Typical example is shown in Figure 7, and three main types may be classified: (i) wet scintillations (± 0.25 to $\pm 1.5 \text{ dB}$) which occur simultaneously with rain-induced fades; (ii) quasi-wet scintillations (± 0.25 to $\pm 3.0 \text{ dB}$) which occur immediately after or before the rain event; (iii) dry scintillation (± 0.5 to $\pm 2.25 \text{ dB}$).

It has been observed that for 36.1 GHz - 4 km link across London, the typical signal variation is 0.14 dB r.s.m. (Villar and Matthews (5)). Assuming same structure constant C_n and outer turbulence $L_0 > 10 \text{ m}$ for 40 GHz - 14 km link, the scaled amplitude is $\pm 0.67 \text{ dB peak}$. This is within the smaller range of our measurement. Greater C_n value in arid climate may contribute to the larger amplitude. For wet type, scattering from rain drops has to be taken into consideration which may add to the variation of the atmospheric refractive index. This may explain

the relatively higher rate of the wet type (0.2 Hz compared with 0.08 - 0.10 Hz for other types).

CONCLUSION

The measured margins required for a given link outage (e.g. 17.5 dB and 2.4 dB due to rain and airborne dust respectively for 1 h per year) reveals that using paths of 14 km at 40 GHz seems to be feasible. Atmospheric turbulence at 40 GHz may reach higher range than in continental climate. Quantative measurement of visibility due to airborne dust is obtained using NIR link.

ACKNOWLEDGEMENT

The authors would like to acknowledge the financial support of King Abdulaziz City for Science and Technology grant AT5-29 and the support of the College of Engineering Research Center Proj. 5/403. Thanks are also due to Professor P.A. Matthews, EE Department, University of Leeds, UK, for his helpful discussion.

REFERENCES

1. Middleton, W.E.K., 1952, "Vision Through the Atmosphere", University of Toronto Press, Toronto, Canada.
2. Ansari, A.J., and Evans, B.G., 1982, "Microwave Propagation in Sand and Dust Storms", *IEE Proc. F.*, **129**, 5, 312-322.
3. Zeuv, V.E., 1982, "Laser Beams in the Atmosphere", Consultants Bureau, New York, USA, 142.
4. Olsen, R.L., Rogers, D.C. and Hodge, D.B., 1978, "The aR^b relation in the calculation of rain attenuation", *IEEE on Ant. and Prop.*, **AP-26**, 318-329.
5. Villar, E. and Matthews, P.A., 1978, "Summary of scintillation observations on a 36 GHz link across London", *IEE Conf. Pub.* **169**, 2, 36-40.

APPENDIX - Explanation of Symbols

Symbol	Explanation
AGC	Automatic gain control voltage.
ADU	Audio signal.
BKM	Microwave link code.
DRO	Dielectric resonant oscillator.
GaAs	Gallium arsenide.
HU/HUP	MMW link codes (first and second).
IF	Intermediate frequency signal.
NEC	MMW link code (third).
SC	Signal conditioner.
VDU	Video signal.
X-Y Rec	Chart recorder.

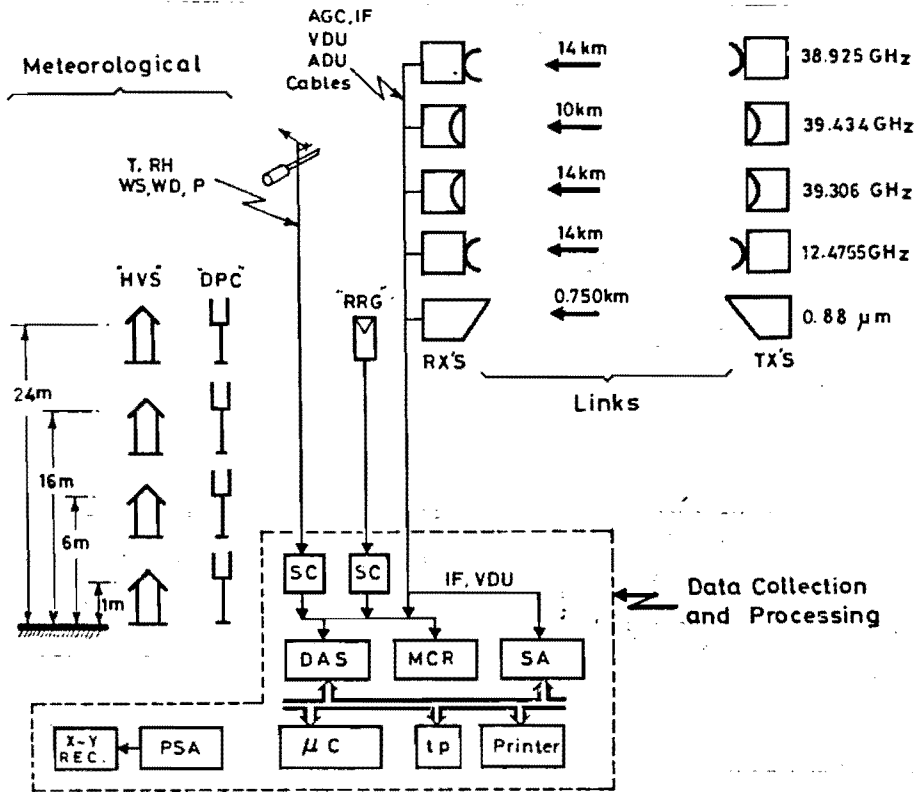


Figure 1. Block diagram of the experimental system (symbols are explained in text).

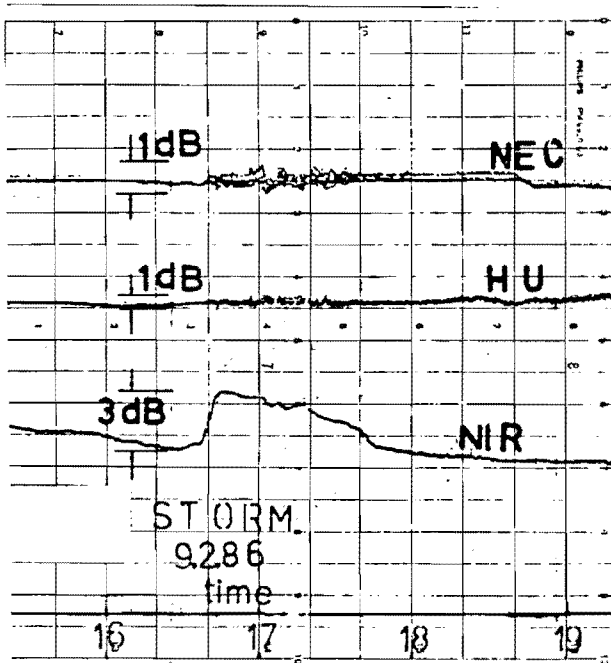


Figure 2. Measured attenuation due to blown dust ($V_0 = 3.75$ km) on MMW and NIR links.

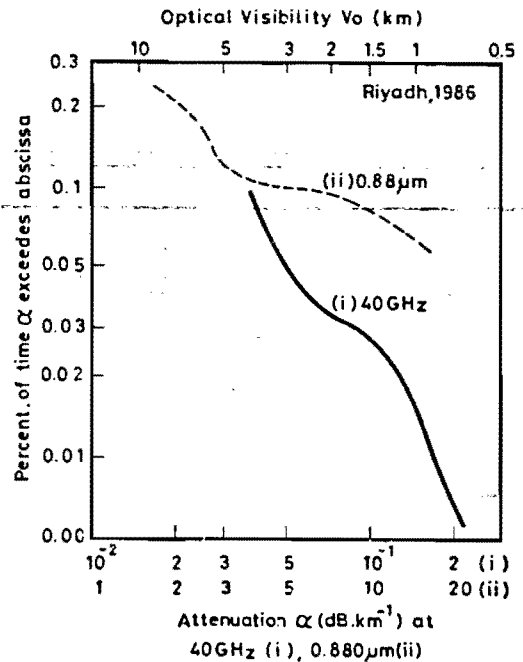


Figure 3. Percentage of time during which dust-attenuation α (dB.km^{-1}) was exceeded.

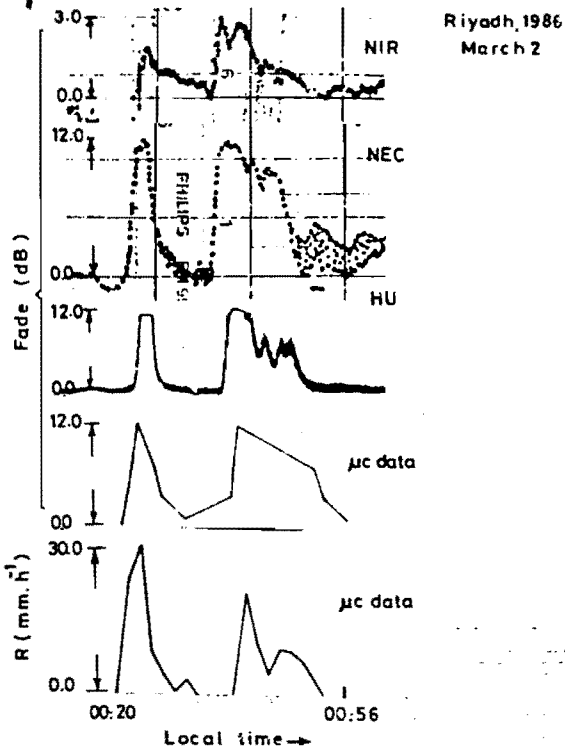


Figure 4. Measured rainfall rate and fades on the MMW and NIR links.

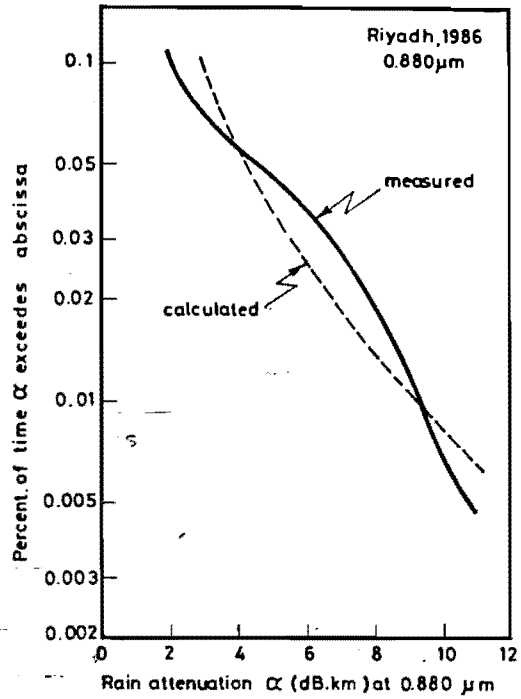


Figure 5. Percentage of time during which rain attenuation α_0 (dB.km^{-1}) was exceeded at $0.880 \mu\text{m}$.

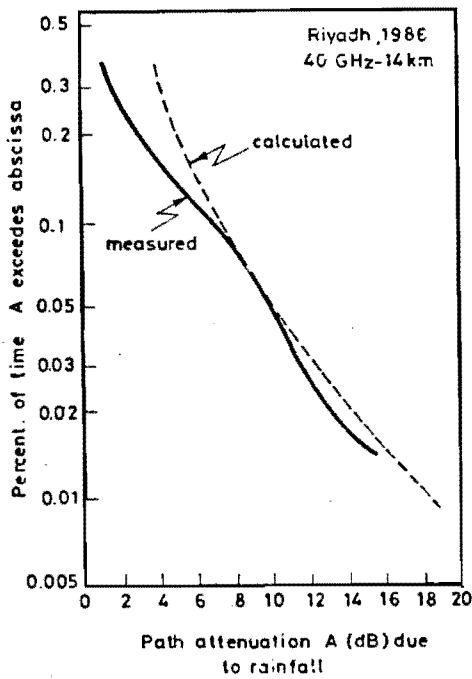


Figure 6. Percentage of time during which path attenuation A (dB) was exceeded due to rain at 40 GHz.

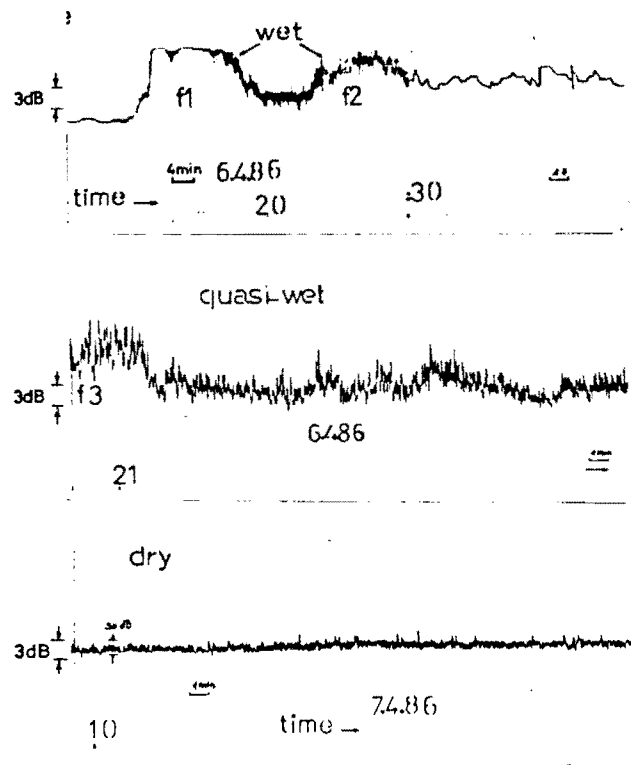


Figure 7. Example of measured types of amplitude scintillation on the MMW link. (f_1 , f_2 are fades numbers)